

Article

Synthesis and Biological Evaluation of Dipeptide-Based Stilbene Derivatives Bearing a Biheterocyclic Moiety as Potential Fungicides

Yongchuang Zhu ¹, Xingdong Lin ², Lan Wen ² and Daohang He ^{2,*}¹ School of Chemical Engineering and Technology, Guangdong Industry Polytechnic, Guangzhou 510300, China² School of Chemistry and Chemical Engineering, South China University of Technology, Guangzhou 510640, China

* Correspondence: cehdh@scut.edu.cn; Tel.: +86-20-8711-0234

Abstract: The escalating demand for crop production, environmental protection, and food safety warrants the development of new fungicides with greater efficiency, environmental friendliness, and innocuous metabolites to fight against destructive phytopathogens. Herein, we report on the synthesis and antifungal activity of dipeptide-based stilbene derivatives bearing a thiophene-substituted 1,3,4-oxadiazole fragment for the first time. In vitro bioassay indicated that the target compounds had remarkable antifungal potency superior to previously reported counterparts without a dipeptidyl group, of which compound **3c** exhibited the highest activity against *Botrytis cinerea* with EC₅₀ values of 106.1 µg/mL. Moreover, the in vivo protective effect of compound **3c** (59.1%) against tomato gray mold was more potent than that of carboxin (42.0%). Preliminary investigations on the mode of action showed that compound **3c** induced marked hyphal malformations and increased the membrane permeability of *B. cinerea* as well as inhibiting mycelial respiration. These promising results suggest that this novel type of molecular framework has great potential to be further developed as alternative fungicides.

Keywords: stilbene; dipeptide; 1,3,4-oxadiazole; thiophene; antifungal activity; mechanism



Citation: Zhu, Y.; Lin, X.; Wen, L.; He, D. Synthesis and Biological Evaluation of Dipeptide-Based Stilbene Derivatives Bearing a Biheterocyclic Moiety as Potential Fungicides. *Molecules* **2022**, *27*, 8755. <https://doi.org/10.3390/molecules27248755>

Academic Editors: Marijana Radić Stojković, Ivo Crnolatac and Lidija-Marija Tumor

Received: 24 October 2022

Accepted: 6 December 2022

Published: 9 December 2022

Publisher's Note: MDPI stays neutral with regard to jurisdictional claims in published maps and institutional affiliations.



Copyright: © 2022 by the authors. Licensee MDPI, Basel, Switzerland. This article is an open access article distributed under the terms and conditions of the Creative Commons Attribution (CC BY) license (<https://creativecommons.org/licenses/by/4.0/>).

1. Introduction

Plant fungal infections have remarkably brought about yield reduction and product deterioration as primary plant diseases that have resulted in economic losses in crops [1]. Especially, *Botrytis cinerea* is among the top-ten phytopathogenic fungi given scientific or economic importance, as it causes damage during plant cultivation as well as after harvest [2–4]. *B. cinerea*, known as gray mold, is intractable because of its broad host range of more than 220 eudicot plants and manifold attack strategies that include cell wall-degrading enzymes, phytotoxins, and detoxification proteins [5,6]. Several characteristics of chemical fungicides, consisting of low cost, high efficiency, rapid action, and long efficacy duration, remain the mainstay of fungal disease control. Nevertheless, it is the appearance of drug-resistant pathogens [7], and environmental residuals toxic to other organisms [8] resulting from inappropriate or long-term use of available chemicals, that warrant the development of antifungal surrogates with an innovative framework, outstanding bioactivity, and good biocompatibility.

In this context, extensive research efforts have been focused on the exploitation of natural products as an inestimable source of prospective candidates with new modes of action and reasonable degradability. Stilbenes possessing a 1,2-diphenylethylene backbone, a group of plant secondary metabolites, such as well-known resveratrol, are involved in plant defense against multiple biotic and abiotic stresses [9]. Their biological activities [10] and clinical potential [11] have been elaborately documented in the literature. However, although they could inhibit phytopathogenic fungal growth in vitro [12,13], the paucity [10,14], rapid oxidation, and microbial metabolism [15,16] of naturally occurring

stilbenes make their external applications on crops hard to achieve, and therefore necessitate synthesis and modification of chemical mimics. Heterocyclic compounds are widely used as components of many biologically active molecules for the optimization of lead compounds in drug development. Thereinto, 1,3,4-oxadiazole substructure prevalent in pesticides and drugs is commonly integrated into the target structures to innovate their biopharmaceutical activities, including antimicrobial [17], anti-inflammatory [18], antitumor [19], and anti-diabetic [20] activities. As another privileged building block, thiophene moiety has drawn the considerable interest of researchers since its derivatives show appreciable diversity in biological effects, such as insecticidal [21], fungicidal [22], and herbicidal [23] effects. Thus, exploration of stilbene backbone modified by these molecular motifs should be expected.

Due to the important role of peptides in living organisms, peptides have been reported as resourceful pharmacological vehicles, and to date, more than 60 peptide therapies have been approved in the United States and other major markets [24–26]. Moreover, dipeptide agents, the shortest peptides, are not only easy to prepare and devoid of toxic metabolites, but they are capable of penetrating biological barriers and are more stable when compared to oligopeptides [27]. Dipeptide derivatives, natural and synthetic, have been investigated for applications in diverse aspects [28–31]. For example, the cyclic Leu-leu dipeptide was isolated and purified from the ethyl acetate extract of a broth of the genus *Gordonia* sp. (WA4-31). Antibacterial experiments showed that it had good inhibitory effects on *Candida albicans*, *Aspergillus niger*, and so on [32]. Khalaf et al. reported Gly-Gly dipeptide derivatives as effective inhibitors against *Bacillus subtilis* and *Candida albicans* [33].

In a previous study, we synthesized a series of 5-(2-thienyl)-1,3,4-oxadiazole-containing stilbene derivatives that displayed promising antifungal activities and could be considered as a potential bioactive scaffold [34]. As a part of our ongoing efforts to develop novel stilbenes of potent fungicidal competence, three different dipeptide fragments (Gly-Gly, Gly-Met, Gly-Leu) were integrated into this stilbene scaffold based on the molecular hybridization principle. The newly synthesized substances were first screened for their *in vitro* antifungal activities against *B. cinerea*. In addition, their *in vivo* protective efficacies against tomato gray mold were tested to explore their practical potential in agriculture. The antifungal mechanism of these designed molecules was preliminarily studied in terms of hyphal morphology, membrane permeability, and mycelial respiration.

2. Results and Discussion

2.1. Chemistry

Preparation of target compounds **3a–3c** was achieved as depicted in Figure 1 starting from the previously described heterocyclic-substituted benzylphosphonate. The stilbene was obtained by the Wittig–Horner reaction of compound **1** with *p*-(Methoxycarbonyl)benzaldehyde, followed by basic hydrolysis to restore the carboxylic acid functionality. The condensation reaction with glycine in the presence of HOBt and EDCI to provide amide was next, which was finally coupled with a certain L-amino acid under the same conditions as one of the former steps for forming the peptide linkage. It is noteworthy that the whole experiment proceeded smoothly without laborious column chromatographic purification, and the target compounds were obtained in good yields. The structures of newly synthesized compounds were confirmed by NMR and HRMS spectral analysis.

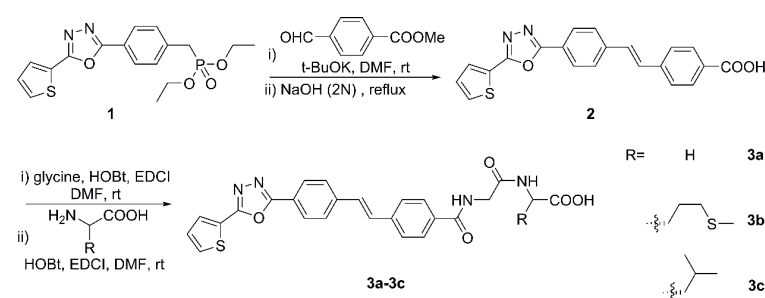


Figure 1. Synthetic route for the target molecules **3a–3c**.

2.2. In Vitro Antifungal Activities

For the required compounds, the bactericidal activity against two important fungal pathogens was evaluated in vitro. These compounds were preliminarily evaluated at 200 µg/mL, and successfully, the evaluation results (Table 1) revealed that the synthesized molecules showed moderate to good inhibition effects toward the tested fungi. The EC₅₀ values for dipeptidyl stilbene derivatives, along with the commercial amide fungicide carboxin, were measured for further exploration of their antifungal potential and are listed in Table 1. It can be clearly seen that compounds **3a–3c** were all more potent against *B. cinerea*, with EC₅₀ values ranging from 106.1 to 119.6 µg/mL compared to carboxin (EC₅₀ = 138.7 µg/mL), out of which **3c** presented the highest level of activity (EC₅₀ = 106.1 µg/mL) and was over twice more effective than resveratrol (EC₅₀ = 263.1 µg/mL). Despite having less potency against *C. lagenarium*, compounds **3b** and **3c** still exerted fungicidal performance comparable to or better than that of the positive control carboxin. For instance, the EC₅₀ value of **3c** was 186.7 µg/mL, lower than that of carboxin (EC₅₀ = 201.7 µg/mL). There was an interesting phenomenon in that the final integrated structures displayed growing inhibitory activities with the increasing hydrophobicity of dipeptide substituents due to changes of the external exposed amino acid (Gly < Met < Leu [35]). Furthermore, in contrast with our previous work where the best compound inhibited *B. cinerea* in vitro with EC₅₀ = 155.4 µg/mL [36], this test outcome indicated that the introduction of simple dipeptidyl moiety was beneficial to antifungal action.

Table 1. In vitro antifungal activities of the target compounds against *B. cinerea*.

Compound	Inhibition Rate (%) at 200 µg/mL ^a	EC ₅₀ (µg/mL)
3a	73.0 ± 1.2 b	119.6
3b	74.8 ± 1.7 b	116.3
3c	79.6 ± 2.6 a	106.1
Carboxin	77.9 ± 1.6 ab	138.7
Resveratrol ^b	44.5 ± 1.2 c	263.1

^a Means followed by different letters within each column are significantly different (Tukey's test, $p < 0.05$). ^b Data from our previous report under the same test conditions [36].

2.3. Effect on Gray Mold of Tomatoes

Inspired by the ameliorated antifungal activities of the target compounds in the in vitro assay, an in vivo experiment for these molecules against tomato gray mold was carried out to examine their practical potential, and the obtained results are summarized in Table 2. The inhibitory effects of synthetic compounds against *B. cinerea* in vivo were identical to those observed against mycelial growth in the Petri dishes. Compounds **3a–3c** exhibited excellent protective impacts with the control efficacy of 55.2%, 56.1%, and 59.1%, respectively, at a concentration of 400 µg/mL. Meanwhile, they were all more effective than carboxin (42.0%), among which **3c** can availablely prevent the extension of lesions on tomatoes, as is illustrated in Figure 2. Considering the unique chemical structure and efficient bioactivities of dipeptidyl stilbene derivatives containing heterocycles, it is suggested that this type of molecular scaffold could be regarded as prospective agrochemicals for the management of *B. cinerea*.

Table 2. Protective activities of compounds **3a–3c** against tomato gray mold at 400 µg/mL under greenhouse conditions.

Compound	Lesion Length (mm) ^a	Control Efficacy (%)
3a	24.7 ± 2.6 c	55.2%
3b	24.3 ± 1.3 c	56.1%
3c	23.0 ± 1.5 c	59.1%
Carboxin	30.5 ± 1.4 b	42.0%
Resveratrol	25.0 ± 2.2 c	54.5%
CK ^b	49.0 ± 1.0 a	

^a Results are means of three independent replicates ± SD; means with different letters are significantly different (Tukey's test, $p < 0.05$). ^b Blank Control.

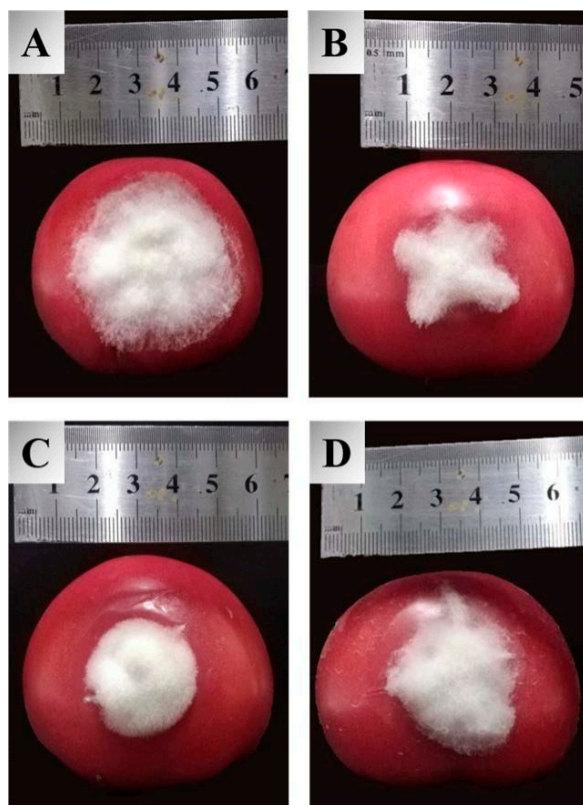


Figure 2. Protective efficacy of compound **3c**, resveratrol, and carboxin against tomato gray mold at 400 µg/mL, (A) blank control, (B) **3c**, (C) resveratrol, (D) carboxin.

2.4. Optical Microscopy Analysis

The hyphal morphological alterations of *B. cinerea* in response to treatment with **3c** were monitored by light microscopy. In the control sample, the hyphae appeared linear and intact tubular, and homogenous with distinguishable septa, while as shown in Figure 3B, the fungus subjected to the action of compound **3c** at 100 µg/mL presented evident changes, of which hyphal vesiculation was particularly visible. The imprints on the mycelia were more significant after exposure to 200 µg/mL **3c**, and microscopic examination showed irregularly tortuous hyphae without a relatively uniform diameter, swollen or elongated. These observed mycelial malformations implied that destroying the structure of the cell wall and membrane system might be one of the antifungal mechanisms of compound **3c** against *B. cinerea*.

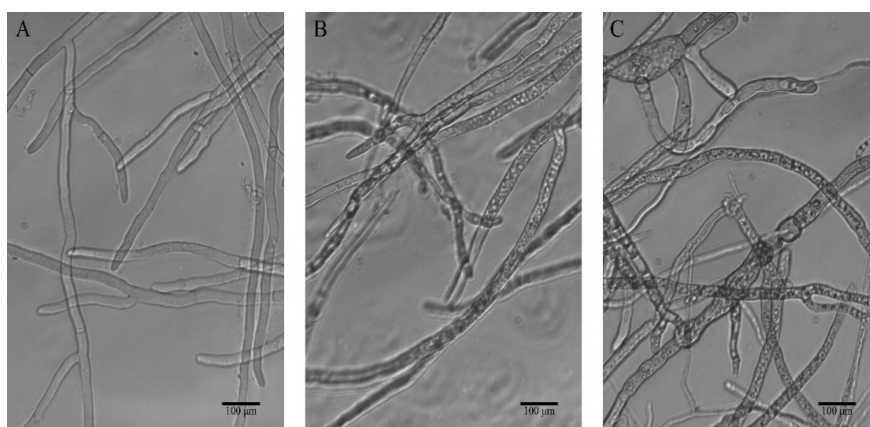


Figure 3. Effect of different concentrations of compound **3c** on the hyphal morphology of *B. cinerea* strains observed by a light microscope ($\times 200$), (A) blank control, (B) 100 µg/mL, (C) 200 µg/mL.

2.5. Effect on Cell Membrane Permeability

Cell membrane plays a pivotal role in maintaining cellular basic metabolism and defending the cell against exogenous disturbance [36]. Electrolyte leakage is generally taken as an indicator of cell membrane permeability. Hence, in order to confirm whether compound **3c** affects the membrane permeability of *B. cinerea*, the electrical conductivity of suspensions of intact mycelia was measured. Compared to the control group, the relative permeability in the **3c**-treated groups was higher and continually elevated during the entire time of treatment, even 25 h later (Figure 4). Besides, the extent of the damage induced by **3c** to the mycelial cell membrane system increased in a concentration-dependent manner, which was distinctly revealed by significant effects at 200 µg/mL within 10 h. These findings proved that the exposure to compound **3c** permeabilized the membrane, led to electrolyte leakage and thereby augmented the conductivity of the solution.

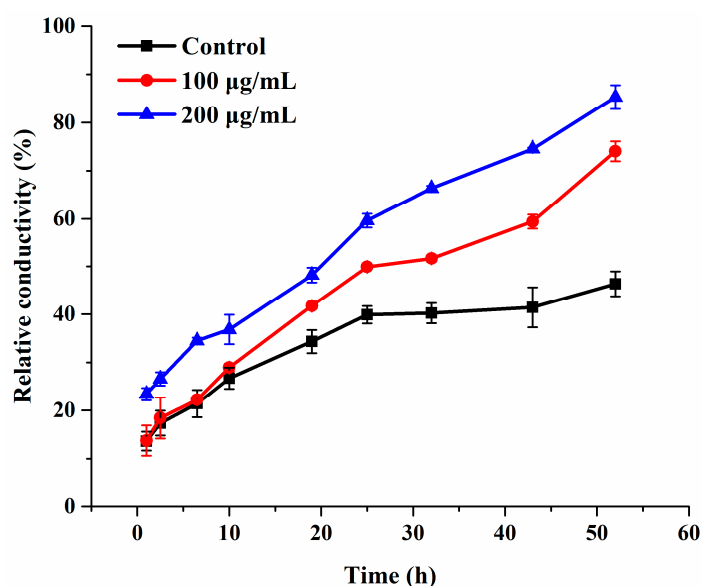


Figure 4. Electrolyte leakage from *B. cinerea* suspensions treated with compound **3c**. Each treatment was carried out in triplicate.

2.6. Effect on Mycelial Respiration

According to related reports, pterostilbene can interact with the mitochondrial membrane of cells and inhibit cell respiration [37]. To further explore the antifungal mechanism, we tested the mycelial oxygen consumption rate of *B. cinerea* when treated with compound **3c**, utilizing a respiration inhibitor, boscalid, as a reference. Notwithstanding that the respiration inhibitory activity ($58.8 \pm 5.9\%$) was poorer than that of boscalid ($82.8 \pm 1.2\%$) at an equal dose (Figure 5), treatment with **3c** had a statistically significant impact on mycelial respiration, which suggested that this compound might also function in the same way as boscalid and partly suppress the mycelium growth of *B. cinerea* by inhibiting the mitochondrial respiratory chain. Likewise, the low level of compound **3c** resulted in less prominent inhibition of oxygen consumption. Combined with the results of the membrane permeability assay, it was inferred that **3c** exerted antifungal activity against *B. cinerea* through multiple pathways, favorable to retarding the development of fungal resistance.

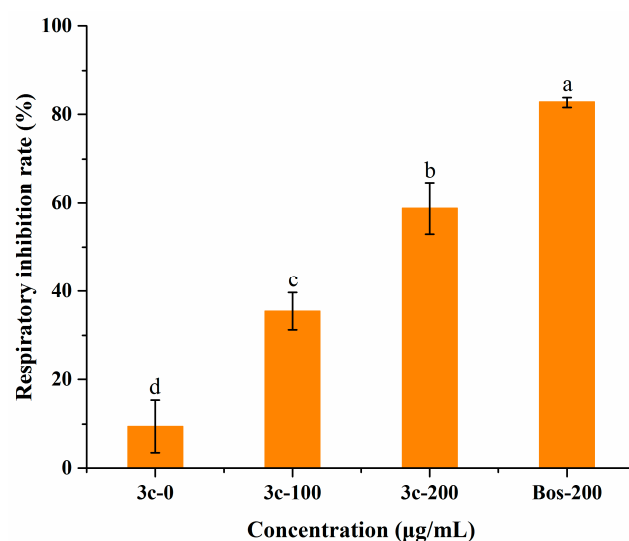


Figure 5. Evaluation of the respiratory inhibition rate on *B. cinerea* mycelia exposed to compound **3c** and the commercial respiration inhibitor boscalid (BOS). Different letters among treatments mean statistically significant differences using Tukey's test ($p < 0.05$).

To sum up, we designed and synthesized structurally tunable dipeptide-based stilbene derivatives bearing thiophene and 1,3,4-oxadiazole moieties by innovatively introducing easy-to-prepare and diverse dipeptides. The *in vitro* bioassay indicated that all the compounds possessed better fungicidal activities against tested fungal strains than that of resveratrol. Furthermore, *in vivo* experiments demonstrated their effectiveness for the control of tomato gray mold caused by *B. cinerea*. It was also observed that abnormal hyphal morphology, increased membrane permeability, and the repressed mycelial respiration of *B. cinerea* took place after interaction with compound **3c**. Given their high efficacies and versatile effects on gray mold, dipeptidyl stilbenes are of promising development value for seeking novel agricultural fungicides.

3. Materials and Methods

3.1. Chemicals and Instrumentation

All chemicals, reagents, and solvents were obtained commercially and used without further purification. Melting points were determined employing a BUCHI Melting Point M-565. ^1H , and ^{13}C NMR spectra were recorded in deuterated dimethyl sulfoxide ($\text{DMSO-}d_6$) on a Bruker AVANCE 400 (400 MHz for ^1H and 100 MHz for ^{13}C) spectrometer (Switzerland) using TMS as an internal standard. Chemical shifts (δ) were expressed in parts per million (ppm) and coupling constants (J) were given in hertz (Hz). The following abbreviations were used to explain the multiplicities: s = singlet; d = doublet; t = triplet; q = quartet; m = multiplet. Mass spectra were registered on a high-resolution electrospray ionization mass spectrometer (maXis impact, Bruker, Germany).

3.2. *In Vitro* Antifungal Test

The *in vitro* fungicidal activity of the target compounds was demonstrated by examining the inhibition of the mycelial radial growth of representative phytopathogenic fungus, *B. cinerea*. These compounds were initially diluted to the testing concentration of 200 $\mu\text{g/mL}$ with PDA medium at 50–60 $^\circ\text{C}$ and transferred into sterilized Petri dishes. After solidification, 5 mm-diameter mycelial disks taken from the peripheral part of a colony of each active fungus were placed at the center of the dishes aseptically. The plates were then incubated at 25 $^\circ\text{C}$ for 3 days. DMSO served as the negative control whereas carboxin served as the positive control. Each experiment was carried out in triplicate. The inhibitory effect of the test compounds on both fungi was calculated by the formula $I = (1 - a/b) \times 100\%$, where I represented the inhibition rate, and a and b were the

mean colony diameters in the untreated and treated Petri dishes, respectively. Additionally, the corresponding inhibition rates of all test compounds at a series of concentrations (400, 200, 100, 50, 25, 12.5, 6.25 $\mu\text{g}/\text{mL}$) were measured under the same conditions as described above to compute medium effective concentration (EC_{50}) values with SPSS 17.0 software.

3.3. *In Vivo* Assay against Tomato Gray Mold

In vivo assay was conducted on tomatoes (*Lycopersicon esculentum*) artificially inoculated with *B. cinerea*. Fruits were selected as experimental material based on uniformity and absence of physical injuries or infections, then surfaced-disinfected with 75% ethanol, rinsed with tap water, and air-dried before treatment. Test solutions (400 $\mu\text{g}/\text{mL}$) of synthesized compounds, prepared by dissolution in DMSO and dilution with distilled water comprising 0.1% Tween 80, were sprayed evenly on fruits and allowed to dry at room temperature. Commercial carboxin and an equivalent amount of DMSO were used as controls. The fruits were wounded with a sterile inoculation needle at the equatorial region and inoculated with the pathogen afterward. Each treatment consisted of three replicates. Treated fruits were stored at 25 °C and high relative humidity (90–95%) for one week. The efficacy of test compounds was expressed by the percentage of reduction in lesion diameter that was determined using the cross method.

3.4. Optical Microscopy of Hyphal Morphology of *B. cinerea*

Three-day-old *B. cinerea* mycelia were cultured in 50 mL potato dextrose broth (PDB) containing different concentrations of **3c** (100 $\mu\text{g}/\text{mL}$ and 200 $\mu\text{g}/\text{mL}$). The blank control had equal content (0.5%) of DMSO. After incubation at 25 °C for 22.5 h, the mycelia were collected, washed with 0.2 M phosphate-buffered saline (PBS) at pH 7.2, resuspended in PBS (0.2 M, pH 7.2), and observed using a light microscope at $\times 200$ magnification.

3.5. Assessment of Cell Membrane Permeability

The change in the membrane permeability of *B. cinerea* was examined by measuring relative conductivity with a DDS-307 conductivity meter (Shanghai INESA Scientific Instrument Co. Ltd., Shanghai, China). The mycelia of 3-day-old *B. cinerea* were collected from PDB medium and washed with sterile distilled water, then treated with 100 or 200 $\mu\text{g}/\text{mL}$ compound **3c**. 0.01% DMF at the same dosage as the solutions mentioned above, and served as the blank control. Thereafter, the electrical conductivity of the mycelia suspension was determined at 0 (L_0), 1, 2.5, 6.5, 10, 19, 25, 32, 43, and 52 h (L_1) with the final conductivity (L_2) of mycelia suspension being after it was boiled and cooled. The equation for the relative permeability was $p = [(L_1 - L_0) / (L_2 - L_0)] \times 100\%$.

3.6. Determination of Oxygen Consumption

The influence of compound **3c** on the mycelial respiration of *B. cinerea* was evaluated as stated by Yan et al [38]. Mycelial blocks from a one-week-old culture of *B. cinerea* were placed in 50 mL PDB and incubated at 25 °C for 3 days with 200 rpm shaking. After being harvested and rinsed, mycelia were suspended in 0.1 M PBS (pH 7.2, 50 mg fresh weight of mycelia mL^{-1}) amended with 2% glucose, comprising **3c** (100 or 200 $\mu\text{g}/\text{mL}$) or boscalid (200 $\mu\text{g}/\text{mL}$, positive control) and 0.01% DMF (blank control). Each treatment was repeated three times. A JPB-607A dissolved oxygen meter (Shanghai INESA Scientific Instrument Co. Ltd., Shanghai, China) was employed to determine mycelial oxygen consumption. The inhibition rate of respiration (IR) was calculated by the following formula $I_R = (1 - R_1 / R_0) \times 100\%$, where R_1 and R_0 were the ratios of mycelial oxygen uptake with or without treatment, respectively. Statistical analysis of the results was performed using SPSS 17.0.

3.7. General Method for the Synthesis of Carboxylic Acid 2

Phosphonate **1** (1.89 g, 5 mmol) prepared according to the procedure reported (see Supplementary Materials) was dissolved in DMF (30 mL) and added to a 100 mL flask

containing *p*-(Methoxycarbonyl)benzaldehyde (0.82 g, 5 mmol); then, an ethanol solution of potassium *tert*-butoxide (15 mL, 6 mmol) was introduced and the mixture was stirred for 6 h. The formed precipitate was filtered, washed with water, and dried to obtain intermediate ester.

The hydrolyzation of ester was carried out with 2 N NaOH aqueous solution under reflux (6 h). After cooling to room temperature, the solution was acidified to pH 3–4 with 1 M HCl, followed by filtration to obtain a crude product that was purified by recrystallization from DMSO/EtOH to give 1.31 g of **2**.

3.8. General Method for the Synthesis of the Target Compounds

A two-step synthetic procedure was applied to obtain the target compounds. Acid **2** (1.20 g, 3.20 mmol) was stirred for 2 h in DMF (30 mL) at ambient temperature with 1-hydroxybenzotriazole (HOBt, 0.43 g, 3.20 mmol) and 1-(3-dimethylaminopropyl)-3-ethylcarbodiimide hydrochloride (EDCI, 0.61 g, 3.20 mmol). Glycine (0.24 g, 3.20 mmol) was then added and the reaction system was left to stir for 7 h. Then, 50 mL of water was added and the resultant yellow solid was removed by filtration and washed successively with 0.5 M HCl and methanol to remove impurities.

The coupling of the above resultant with glycine, L-methionine and L-leucine, respectively, was performed in a similar manner to its own synthetic protocols to afford target compounds **3a–3c** that were recrystallized from DMSO/EtOH.

3.8.1. (E)-4-(4-(5-(Thiophen-2-yl)-1,3,4-oxadiazol-2-yl)styryl)benzoic acid (**2**)

^1H NMR (400 MHz, DMSO- d_6) δ 12.91 (s, COOH, 1H), 8.07 (d, J = 8.0 Hz, Th-H, 2H), 7.96 (d, J = 7.5 Hz, Ph-H, 4H), 7.85 (d, J = 8.1 Hz, Ph-H, 2H), 7.75 (d, J = 8.0 Hz, Ph-H, 2H), 7.48 (s, CH = CH, 2H), 7.32 (t, J = 4.3 Hz, Th-H, 1H); ^{13}C NMR (101 MHz, DMSO- d_6) δ 167.46, 163.76, 160.78, 141.38, 140.65, 132.12, 131.00, 130.45, 130.29, 130.24, 130.18, 129.20, 128.05, 127.49, 127.27, 124.76, 122.67; HRMS (ESI), m/z calcd for $\text{C}_{21}\text{H}_{15}\text{N}_2\text{O}_3\text{S}$ [M + H] $^+$ + 375.0798; found, 375.0793.

3.8.2. (E)-4-(4-(5-(Thiophen-2-yl)-1,3,4-oxadiazol-2-yl)styryl)benzoyl)glycylglycine (**3a**)

A yellow solid, yield 54%, mp 217–218 °C; ^1H NMR (400 MHz, DMSO- d_6) δ 12.56 (s, 1H), 8.86 (dt, J = 17.9, 5.7 Hz, 1H), 8.24 (t, J = 5.9 Hz, 1H), 8.12 (d, J = 8.0 Hz, 2H), 7.99 (t, J = 4.0 Hz, 2H), 7.94 (d, J = 8.1 Hz, 2H), 7.89 (d, J = 8.1 Hz, 2H), 7.78 (d, J = 8.1 Hz, 2H), 7.52 (s, 2H), 7.35 (t, J = 4.4 Hz, 1H), 3.94 (d, J = 5.8 Hz, 2H), 3.79 (d, J = 5.8 Hz, 2H); ^{13}C NMR (101 MHz, DMSO- d_6) δ 171.64, 169.83, 166.47, 163.80, 160.80, 140.84, 139.97, 133.71, 132.19, 131.06, 130.47, 129.54, 129.26, 128.39, 127.99, 127.54, 127.06, 124.77, 122.55, 42.93, 41.18; HRMS (ESI) [M + Na] $^+$ calcd for $\text{C}_{25}\text{H}_{20}\text{N}_4\text{O}_5\text{S}$: 511.1047, found: 511.1040.

3.8.3. (E)-4-(4-(5-(Thiophen-2-yl)-1,3,4-oxadiazol-2-yl)styryl)benzoyl)glycyl-L-methionine (**3b**)

A yellow solid, yield 50%, mp 196–197 °C; ^1H NMR (400 MHz, DMSO- d_6) δ 12.61 (s, 1H), 8.76 (t, J = 6.0 Hz, 1H), 8.24 (d, J = 7.9 Hz, 1H), 8.11 (d, J = 8.0 Hz, 2H), 7.98 (t, J = 4.0 Hz, 2H), 7.93 (dd, J = 8.3, 3.4 Hz, 2H), 7.88 (d, J = 8.1 Hz, 2H), 7.77 (d, J = 8.1 Hz, 2H), 7.51 (s, 2H), 7.34 (t, J = 4.4 Hz, 1H), 4.38 (td, J = 8.5, 4.5 Hz, 1H), 4.03–3.89 (m, 2H), 2.55 (s, 4H), 2.05 (s, 3H); ^{13}C NMR (101 MHz, DMSO- d_6) δ 173.67, 169.55, 166.48, 163.80, 160.80, 140.84, 139.95, 133.75, 132.18, 131.06, 130.47, 129.54, 129.26, 128.33, 127.99, 127.54, 127.08, 124.76, 122.55, 51.41, 40.90, 31.30, 30.11, 15.05; HRMS (ESI) [M + H] $^+$ calcd for $\text{C}_{28}\text{H}_{27}\text{N}_4\text{O}_5\text{S}_2$: 563.1378, found: 563.1418.

3.8.4. (E)-4-(4-(5-(Thiophen-2-yl)-1,3,4-oxadiazol-2-yl)styryl)benzoyl)glycyl-L-leucine (**3c**)

A yellow solid, yield 56%, mp 215–216 °C; ^1H NMR (400 MHz, DMSO- d_6) δ 12.68 (s, 1H), 8.85–8.71 (m, 1H), 8.18 (d, J = 8.1 Hz, 1H), 8.12 (s, 2H), 7.99 (d, J = 5.0 Hz, 2H), 7.93 (d, J = 7.1 Hz, 2H), 7.88 (d, J = 8.0 Hz, 2H), 7.77 (d, J = 5.8 Hz, 2H), 7.51 (s, 2H), 7.34 (d, J = 4.4 Hz, 1H), 4.29 (td, J = 8.6, 5.9 Hz, 1H), 3.96 (t, J = 4.5 Hz, 2H), 1.67 (q, J = 6.8 Hz, 1H), 1.54 (dq, J = 12.6, 7.9, 6.4 Hz, 2H), 0.89 (dd, J = 16.2, 6.5 Hz, 6H); ^{13}C NMR (101 MHz, DMSO- d_6) δ

174.49, 171.82, 169.38, 166.46, 163.80, 160.79, 140.84, 139.93, 133.79, 133.54, 132.18, 131.06, 130.44, 129.25, 128.32, 128.24, 127.99, 127.54, 127.15, 127.08, 124.77, 122.55, 24.76, 23.33, 21.91; HRMS (ESI) $[M + H]^+$ calcd for $C_{29}H_{29}N_4O_5S$: 545.1814, found: 545.1856.

Supplementary Materials: The following supporting information can be downloaded at: <https://www.mdpi.com/article/10.3390/molecules27248755/s1>, Synthetic procedure and characterization data for intermediate 1, citation of references [34,39]

Author Contributions: Conceptualization, Y.Z. and D.H.; methodology, X.L.; software, X.L.; validation, L.W., Y.Z. and D.H.; formal analysis, X.L.; investigation, Y.Z.; resources, X.L.; data curation, L.W.; writing—original draft preparation, Y.Z.; writing—review and editing, D.H.; visualization, X.L.; supervision, D.H.; project administration, Y.Z.; funding acquisition, D.H. All authors have read and agreed to the published version of the manuscript.

Funding: This work was financially supported by the Natural Science Foundation of Guangdong Province (2018A030313224).

Institutional Review Board Statement: Not applicable.

Informed Consent Statement: Not applicable.

Data Availability Statement: Data is contained within the article.

Conflicts of Interest: The authors declare no competing financial interests.

Sample Availability: Samples of the compounds are not available from the authors.

References

1. Horbach, R.; Navarro-Quesada, A.R.; Knogge, W.; Deising, H.B. When and how to kill a plant cell: Infection strategies of plant pathogenic fungi. *J. Plant Physiol.* **2011**, *168*, 51–62. [[CrossRef](#)] [[PubMed](#)]
2. Dean, R.; Van Kan, J.A.L.; Pretorius, Z.A.; Hammond-Kosack, K.E.; Di Pietro, A.; Spanu, P.D.; Rudd, J.J.; Dickman, M.; Kahmann, R.; Ellis, J.; et al. The Top 10 fungal pathogens in molecular plant pathology. *Mol. Plant Pathol.* **2012**, *13*, 414–430. [[CrossRef](#)] [[PubMed](#)]
3. Liu, X.; Zheng, X.J.; Khaskheli, M.I.; Sun, X.F.; Chang, X.L.; Gong, G.S. Identification of *Colletotrichum* species associated with blueberry anthracnose in Sichuan, China. *Pathogens*. **2020**, *9*, 718. [[CrossRef](#)] [[PubMed](#)]
4. Noor, N.M.; Zakaria, L. Identification and characterization of *Colletotrichum* spp. associated with chili anthracnose in peninsular Malaysia. *Eur. J. Plant Pathol.* **2018**, *151*, 961–973. [[CrossRef](#)]
5. Fournier, E.; Gladioux, P.; Giraud, T. The ‘Dr Jekyll and Mr Hyde fungus’: Noble rot versus gray mold symptoms of *Botrytis cinerea* on grapes. *Evol. Appl.* **2013**, *6*, 960–969. [[CrossRef](#)]
6. Han, S.H.; Song, M.H.; Keum, Y.S. Effects of azole fungicides on secreted metabolomes of *Botrytis cinerea*. *J. Agric. Food Chem.* **2020**, *68*, 5309–5317. [[CrossRef](#)]
7. Veloukas, T.; Markoglou, A.N.; Karaoglaniadis, G.S. Differential effect of SdhB gene mutations on the sensitivity to SDHI fungicides in *Botrytis cinerea*. *Plant Dis.* **2013**, *97*, 118–122. [[CrossRef](#)]
8. Chambers, J.E.; Greim, H.; Kendall, R.J.; Segner, H.; Sharpe, R.M.; Van Der Kraak, G. Human and ecological risk assessment of a crop protection chemical: A case study with the azole fungicide epoxiconazole. *Crit. Rev. Toxicol.* **2014**, *44*, 176–210. [[CrossRef](#)]
9. Shen, T.; Wang, X.N.; Lou, H.X. Natural stilbenes: An overview. *Nat. Prod. Rep.* **2009**, *26*, 916–935. [[CrossRef](#)]
10. Singh, D.; Mendonsa, R.; Koli, M.; Subramanian, M.; Nayak, S.K. Antibacterial activity of resveratrol structural analogues: A mechanistic evaluation of the structure-activity relationship. *Toxicol. Appl. Pharmacol.* **2019**, *367*, 23–32. [[CrossRef](#)]
11. Roupe, K.A.; Remsberg, C.M.; Yanez, J.A.; Davies, N.M. Pharmacometrics of stilbenes: Seguing towards the clinic. *Curr. Clin. Pharmacol.* **2006**, *1*, 81–101. [[CrossRef](#)] [[PubMed](#)]
12. Xu, D.D.; Deng, Y.Z.; Han, T.Y.; Jiang, L.Q.; Xi, P.G.; Wang, Q.; Jiang, Z.D.; Gao, L.W. In vitro and in vivo effectiveness of phenolic compounds for the control of postharvest gray mold of table grapes. *Postharvest Biol. Technol.* **2018**, *139*, 106–114. [[CrossRef](#)]
13. Gabaston, J.; Richard, T.; Biais, B.; Waffo-Teguo, P.; Pedrot, E.; Jourdes, M.; Corio-Costet, M.F.; Mérillon, J.M. Stilbenes from common spruce (*Picea abies*) bark as natural antifungal agent against downy mildew (*Plasmopara viticola*). *Ind. Crop. Prod.* **2017**, *103*, 267–273. [[CrossRef](#)]
14. Wang, Y.; Catana, F.; Yang, Y.N.; Roderick, R.; van Breemen, R.B. An LC-MS method for analyzing total resveratrol in grape juice, cranberry juice, and in wine. *J. Agric. Food Chem.* **2002**, *50*, 431–435. [[CrossRef](#)]
15. De Filippis, B.; Ammazalorso, A.; Amoroso, R.; Giampietro, L. Stilbene derivatives as new perspective in antifungal medicinal chemistry. *Drug Dev. Res.* **2019**, *80*, 285–293. [[CrossRef](#)]
16. Sbaghi, M.; Jeandet, P.; Bessis, R.; Leroux, P. Degradation of stilbene-type phytoalexins in relation to the pathogenicity of *Botrytis cinerea* to grapevines. *Plant Pathol.* **1996**, *45*, 139–144. [[CrossRef](#)]

17. Tao, Q.Q.; Liu, L.W.; Wang, P.Y.; Long, Q.S.; Zhao, Y.L.; Jin, L.H.; Xu, W.M.; Chen, Y.; Li, Z.; Yang, S. Synthesis and in vitro and in vivo biological activity evaluation and quantitative proteome profiling of oxadiazoles bearing flexible heterocyclic patterns. *J. Agric. Food Chem.* **2019**, *67*, 7626–7639. [[CrossRef](#)] [[PubMed](#)]
18. Zheng, X.J.; Li, C.S.; Cui, M.Y.; Song, Z.W.; Bai, X.Q.; Liang, C.W.; Wan-g, H.Y.; Zhang, T.Y. Synthesis, biological evaluation of benzothiazole derivatives bearing a 1,3,4-oxadiazole moiety as potential anti-oxidant and anti-inflammatory agents. *Bioorg. Med. Chem. Lett.* **2020**, *30*, 127237. [[CrossRef](#)]
19. Sharma, V.; Kumar, R.; Angeli, A.; Supuran, C.T.; Sharma, P.K. Tail approach synthesis of novel benzenesulfonamides incorporating 1,3,4-oxadiazole hybrids as potent inhibitor of carbonic anhydrase I, II, IX, and XII isoenzymes. *Eur. J. Med. Chem.* **2020**, *193*, 112219. [[CrossRef](#)]
20. Bhutani, R.; Pathak, D.P.; Kapoor, G.; Husain, A.; Iqbal, M.A. Novel hybrids of benzothiazole-1,3,4-oxadiazole-4-thiazolidinone: Synthesis, in silico ADME study, molecular docking and in vivo anti-diabetic assessment. *Bioorg. Chem.* **2019**, *83*, 6–19. [[CrossRef](#)]
21. Silverio, M.R.S.; Espindola, L.S.; Lopes, N.P.; Vieira, P.C. Plant natural products for the control of *Aedes aegypti*: The main vector of important arboviruses. *Molecules* **2020**, *25*, 3484. [[CrossRef](#)] [[PubMed](#)]
22. Liu, T.T.; Wu, H.B.; Jiang, H.Y. Thiophenes from *Echinops grijsii* as a preliminary approach to control disease complex of root-knot nematodes and soil-borne fungi: Isolation, activities, and structure-nonphototoxic activity relationship analysis. *J. Agric. Food Chem.* **2019**, *67*, 6160–6168. [[CrossRef](#)] [[PubMed](#)]
23. Wang, B.L.; Shi, Y.X.; Zhan, Y.Z.; Zhang, L.Y.; Zhang, Y.; Wang, L.Z.; Zhang, X.; Li, Y.H.; Li, Z.M.; Li, B.J. Synthesis and biological activity of novel furan/thiophene and piperazine-containing (bis)1,2,4-triazole Mannich bases. *Chin. J. Chem.* **2015**, *33*, 1124–1134. [[CrossRef](#)]
24. Ezugwu, J.A.; Okoro, U.C.; Ezeokonkwo, M.A.; Bhimapaka, C.R.; Okafor, S.N.; Ugwu, D.I.; Ekoh, O.C.; Attah, S.I. Novel Leu-Val based dipeptide as antimicrobial and antimalarial agents: Synthesis and molecular docking. *Front. Chem.* **2020**, *8*, 583926. [[CrossRef](#)] [[PubMed](#)]
25. Day, T.; Greenfield, S.A. Bioactivity of a peptide derived from acetylcholinesterase in hippocampal organotypic cultures. *Exp. Brain Res.* **2004**, *155*, 500–508. [[CrossRef](#)] [[PubMed](#)]
26. Lau, J.L.; Dunn, M.K. Therapeutic peptides: Historical perspectives, current development trends, and future directions. *Bioorg. Med. Chem.* **2018**, *26*, 2700–2707. [[CrossRef](#)]
27. Gudasheva, T.A. Theoretical grounds and technologies for dipeptide drug development. *Russ. Chem. Bull.* **2015**, *64*, 2012–2021. [[CrossRef](#)]
28. Miao, J.Y.; Guo, H.X.; Chen, F.L.; Zhao, L.C.; He, L.P.; Ou, Y.W.; Huang, M.M.; Zhang, Y.; Guo, B.Y.; Cao, Y.; et al. Antibacterial effects of a cell-penetrating peptide isolated from Kefir. *J. Agric. Food Chem.* **2016**, *64*, 3234–3242. [[CrossRef](#)]
29. Tareq, F.S.; Lee, M.A.; Lee, H.-S.; Lee, Y.-J.; Lee, J.S.; Hasan, C.M.; Islam, M.T.; Shin, H.J. Gageotettrins A-C, noncytotoxic antimicrobial linear lipopeptides from a marine bacterium *Bacillus subtilis*. *Org. Lett.* **2014**, *16*, 928–931. [[CrossRef](#)]
30. Khan, F.A.; Nasim, N.; Wang, Y.; Alhazmi, A.; Sanam, M.; Ul-Haq, Z.; Yalamati, D.; Ulanova, M.; Jiang, Z.H. Amphiphilic desmuramyl peptides for the rational design of new vaccine adjuvants: Synthesis, in vitro modulation of inflammatory response and molecular docking studies. *Eur. J. Med. Chem.* **2021**, *209*, 112863. [[CrossRef](#)]
31. Lu, X.; Jia, C.; Gao, J.H.; Wang, R.D.; Zhang, L.X.; Sun, Q.; Huang, J.N. Structure-activity relationship and molecular docking analysis of cysteine-containing dipeptides as antioxidant and ACE inhibitory. *Int. J. Food Sci. Technol.* **2020**, *56*, 2789–2803. [[CrossRef](#)]
32. Ma, Y.; Xu, M.H.; Liu, H.C.; Yu, T.T.; Guo, P.; Liu, W.B.; Jin, X.B. Antimicrobial compounds were isolated from the secondary metabolites of gordonia, a resident of intestinal tract of *Periplaneta americana*. *AMB Express* **2021**, *11*, 111. [[CrossRef](#)] [[PubMed](#)]
33. Khalaf, H.S.; Naglah, A.M.; Al-Omar, M.A.; Moustafa, G.O.; Awad, H.M.; Bakheit, A.H. Synthesis, docking, computational studies, and antimicrobial evaluations of new dipeptide derivatives based on nicotinoylglycylglycine hydrazide. *Molecules* **2020**, *25*, 3589. [[CrossRef](#)]
34. Wen, L.; Jian, W.L.; Shang, J.B.; He, D.H. Synthesis and antifungal activities of novel thiophene-based stilbene derivatives bearing an 1,3,4-oxadiazole unit. *Pest Manag. Sci.* **2019**, *75*, 1123–1130. [[CrossRef](#)]
35. Monera, O.D.; Sereda, T.J.; Zhou, N.E.; Kay, C.M.; Hodges, R.S. Relationship of sidechain hydrophobicity and α -helical propensity on the stability of the single-stranded amphipathic α -helix. *J. Pept. Sci.* **1995**, *1*, 319–329. [[CrossRef](#)]
36. Liu, G.S.; Zhang, S.; Yang, K.; Zhu, L.Z.; Lin, D.H. Toxicity of perfluorooctane sulfonate and perfluorooctanoic acid to *Escherichia coli*: Membrane disruption, oxidative stress, and DNA damage induced cell inactivation and/or death. *Environ. Pollut.* **2016**, *214*, 806–815. [[CrossRef](#)] [[PubMed](#)]
37. Serazetdinova, L.; Oldach, K.H.; Lörz, H. Expression of transgenic stilbene synthases in wheat causes the accumulation of unknown stilbene derivatives with antifungal activity. *J. Plant Physiol.* **2005**, *162*, 985–1002. [[CrossRef](#)]
38. Yan, X.J.; Liang, X.M.; Jin, S.H.; Lv, J.P.; Yu, C.X.; Qi, W.Y.; Li, B.J.; Yuan, H.Z.; Qi, S.H.; Shi, Y.X.; et al. Primary study on mode of action for macrocyclic fungicide candidates (7B3, D1) against *Rhizoctonia solani* Kühn. *J. Agric. Food Chem.* **2010**, *58*, 2726–2729. [[CrossRef](#)]
39. Jian, W.L.; He, D.H.; Xi, P.G.; Li, X.W. Synthesis and biological evaluation of novel fluorine-containing stilbene derivatives as fungicidal agents against phytopathogenic fungi. *J. Agric. Food Chem.* **2015**, *63*, 9963–9969. [[CrossRef](#)] [[PubMed](#)]